A Numerical World Ocean General Circulation Model

Zhang Xuehong (张学洪) and *Liang Xinzhong* (梁信忠)
Institute of Atmospheric Physics, Academia Sinica, Beijing
Received April 22, 1988

ABSTRACT

This paper describes a numerical model of the world ocean based on the fully primitive equations. A "Standard" ocean state is introduced into the equations of the model and the perturbed thermodynamic variables are used in the model's calculations. Both a free upper surface and a bottom topography are included in the model and a sigma coordinate is used to normalize the model's vertical component. The model has four unevenly-spaced layers and 4 × 5 horizontal resolution based on C-grid system. The finite-difference scheme of the model is designed to conserve the gross available energy in order to avoid fictitious energy generation or decay.

The model has been tested in response to the annual mean surface wind stress, sea level air pressure and sea level air temperature as a preliminary step to its further improvement and its coupling with a global atmospheric general circulation model. Some of results, including currents, temperature and sea surface elevation simulated by the model are presented.

I. INTRODUCTION

The earth's climate and its variation are the consequence of the interaction between the components of the climate system, including the atmosphere, ocean, ice, biosphere and land elements. The heat capacity of the atmosphere is relatively small, equivalent to only about a 2.5m depth of water; thus, its thermal inertia, or resistance to change of temperature, is relatively small compared with that of the ocean of the averaging depth, which is about 4 km. It is necessary to include the ocean on a global scale, therefore, in order to investigate the climate with time scale much longer than a year. However, many aspects of both the atmosphere and the ocean are too complex to be treated in any other way except by large-scale numerical models for the global atmosphere and the world ocean. Pioneering works in this direction have been done by Phillips (1956), Smagorinsky (1963), Arakawa (1966), Bryan (1969) and etc..

From the viewpoint of geophysical fluid dynamics, the atmosphere and the ocean have many aspects of similarities. It was pointed out by Charney (1981) that there is scarcely a fluid dynamic phenomenon in the planetary atmosphere that does not have its counterpart in the ocean and vice versa. Furthermore, the general principles of the computational geophysical fluid dynamics are applicable to the numerical models for both the atmosphere and the ocean and it is even possible to construct universal numerical models for both of them.

On the basis of a series of research works in this field, Zeng (1983) presented a fully coupled atmosphere-ocean numerical general circulation model.The main features of this model are as follows. (1) the perturbed variables related to the "standard status" of the atmosphere and the ocean are introduced into the equations of the model and the corresponding "available energy" is defined; (2) a hybrid sigma coordinate is used in both the atmosphere and the

ocean and inherent consistent interface boundary conditions are given to describe the interactions between the two media; (3) a set of available energy conservation finite-difference schemes are designed to avoid false computational source and sink of energy and mass; and (4) some flexible coefficients are introduced into the computational schemes, which may provide a convenient way for some empirical modifications and speed-up convergence without violating energy conservations. Since that, a two-level atmospheric general circulation model and a barotropic ocean model have been presented in IAP (Zeng et al.,1987), and the nine-level version of the AGCM, on the cooperative research project on CO_2-induced climate change between P.R.C. and U.S.A., has been tuning at SUNY at Stony Brook since 1987.

Following this line, a preliminary performance of a four-level world ocean general circulation model was also fulfilled by Zhang and Liang at Stony Brook. In this paper, a brief description of the ocean model and some results of the annual mean simulation driven by observational atmospheric conditions will be presented. Details of the model's equations and their variant are introduced in Section II. Section III gives the boundary conditions and energy relations of the model. The model's numerical schemes, including grid system, available energy conservative spatial finite-difference scheme and time integration technique, are described in Section IV. In Section V, a speed-up convergence technique based on the so-called "flexible coefficients" is presented and the corresponding results of the annual mean simulation by the ocean model are given.

II. EQUATIONS OF THE MODEL

1. *General Forms of the Equations*

In the spherical surface coordinates, (θ, λ, z, t), the governing equations of oceanic general circulation may be written as,

$$\frac{d\vec{v}}{dt} = -\frac{1}{\rho_0}\nabla p - f^*\vec{k}\times\vec{v} + \frac{\partial}{\partial z}\left(\kappa\frac{\partial\vec{v}}{\partial z}\right) + A_M\left[\Delta\vec{v} + \frac{1-\mathrm{ctg}^2\theta}{a^2}\vec{v} + \frac{2\mathrm{ctg}\theta}{a^2\sin\theta}\vec{k}\times\frac{\partial}{\partial\lambda}\vec{v}\right], \tag{1}$$

$$\frac{dT}{dt} = -\frac{g\alpha_T T}{c_p}w + \frac{\partial}{\partial z}\left(\frac{\kappa}{\delta}\frac{\partial T}{\partial z}\right) + A_H\Delta T, \tag{2}$$

$$\frac{dS}{dt} = \frac{\partial}{\partial z}\left(\frac{\kappa}{\delta}\frac{\partial S}{\partial z}\right) + A_H\Delta S, \tag{3}$$

$$\frac{\partial w}{\partial z} + \frac{1}{a\sin\theta}\left(\frac{\partial v\sin\theta}{\partial\theta} + \frac{\partial u}{\partial\lambda}\right) = 0, \tag{4}$$

$$\rho = \rho(T, S, p), \tag{5}$$

$$\frac{\partial p}{\partial z} = -\rho g. \tag{6}$$

Here S is the salinity(in gm/kg), ρ and ρ_0 are the density of sea water and its reference value respectively, α_T is the coefficient of thermal expansion of sea water, κ is the vertical eddy viscosity coefficient, and A_M and A_H are the lateral eddy diffusivities of mo-

mentum and heat respectively. The delta in (2) and (3) can be 1 or 0, and the case $\delta=0$ implies that the vertical diffusivities should be replaced by the convective adjustment once a unstable density stratification occurs (Bryan, 1969). The other symbols are the same as those used in the IAP AGCM (Zeng, et al., 1987).

The equations are based on the following three important approximations, i.e., the Boussinesq approximation, the hydrostatic approximation and the closure approximation for small-scale motions based on the turbulent viscosity hypothesis, and have the similar form to the most of the oceanic general circulation models in the world except the compression effect on the temperature being included. In order to utilize the finite-difference schemes and numerical techniques applicable to general geophysical fluid developed in IAP, however, we shall make some further treatments of the above governing equations in a similar manner to that used in the IAP AGCM.

2. *Perturbed Thermodynamic Variables*

There are four thermodynamic variables in (1)–(6), i.e., T, S, ρ and p, in which ρ and p are more than three orders of magnitude greater than that of the atmosphere. What are playing a practical role in oceanic motions are, however, only the departures of these variables from their certain "standard" status. In order to avoid the computational error caused by using the original thermodynamic variables, we introduce a set of perturbed variables as follows,

$$\begin{cases} T' \equiv T(\theta,\lambda,z,t) - \tilde{T}(z), \\ S' \equiv S(\theta,\lambda,z,t) - \tilde{S}(z), \\ \rho' \equiv \rho(\theta,\lambda,z,t) - \tilde{\rho}(z), \\ p' \equiv p(\theta,\lambda,z,t) - \tilde{p}(z), \end{cases} \tag{7}$$

where $\tilde{T}(z)$, $\tilde{S}(z)$, $\tilde{\rho}(z)$ and $\tilde{p}(z)$ represent certain standard vertical distributions of T, S, ρ and p respectively (Zeng et al., 1983). In general, the state equation of sea water (5) is a rather complicated nonlinear equation (e.g., see Eckart, 1958). For the purpose of the simulation of oceanic circulation, however, a suitable approximation of (5) is

$$\frac{\rho'}{\rho_0} = -\alpha_T T' + \alpha_S S', \tag{8}$$

where α_T and α_S are the known functions of height z. As a matter of fact, Bryan–Cox formula (Bryan and Cox, 1972) is just such an approximation. Moreover, the use of (8) provides special forms of $\tilde{T}(z)$, $\tilde{S}(z)$ and $\tilde{\rho}(z)$ as well. The standard distribution of pressure, $\tilde{p}(z)$, can be found from the hydrostatic relation and the pressure continuity condition at the sea surface:

$$\begin{cases} \dfrac{\partial \tilde{p}}{\partial z} = -\tilde{\rho} g, \\ \tilde{p}(0) = \tilde{p}_s, \end{cases} \tag{9}$$

where $\tilde{p}_s$ is the standard sea surface air pressure. Thus, we have the hydrostatic relation in perturbed form as follows,

$$\frac{\partial p'}{\partial z} = -\rho' g. \tag{10}$$

The pressure gradient term in the momentum equation can also be replaced by the corresponding perturbed form, i.e.,

$$-\frac{1}{\rho_0}\nabla p = -\frac{1}{\rho_0}\nabla p'. \tag{11}$$

By taking into account of the role of the standard stratification on the perturbed variables, the thermodynamic equation (2) and the salinity conservation equation (3) may be rewritten as,

$$\frac{dT'}{dt} = -\gamma_T w + \frac{\partial}{\partial z}\left(\frac{\kappa}{\delta}\frac{\partial(\tilde{T}+T')}{\partial z}\right) + A_H \Delta T', \tag{12}$$

and

$$\frac{dS'}{dt} = -\gamma_S w + \frac{\partial}{\partial z}\left(\frac{\kappa}{\delta}\frac{\partial(\tilde{S}+S')}{\partial z}\right) + A_H \Delta S', \tag{13}$$

where

$$\gamma_T \equiv \frac{g}{c_p}\alpha_T \tilde{T} + \frac{\partial \tilde{T}}{\partial z}, \tag{14}$$

and

$$\gamma_S \equiv -\frac{\partial \tilde{S}}{\partial z}. \tag{15}$$

3. *Transformations of Coordinates and Variables*

Table 1. Statistics of Ocean Depth (based on 4 × 5 data)

Depth(m)	Number of Points	Percent
0–6000	2132	100.00
1000–6000	1985	90.20
0–50	15	0.70
50–100	16	0.75
100–200	32	1.50
200–500	70	3.28
500–1000	62	2.91

The realistic bottom topography of the world ocean is rather complicated. (See Gates and Nelson, 1975). It has been pointed out that the usual sigma coordinates, which are very popular in atmospheric models, may break down in world ocean models because the variations in topography are comparable to the depth of the fluid itself(Semtner,1986). Fortunately, the data statistics of the world ocean depth shows that the depths of more than 90% of the ocean grid points are greater than 1000 meters (see Table 1). As the first step of

developing IAP world ocean model, therefore, a modified bottom topography and a slightly idealized geography are presented, for which the conventional sigma coordinates are feasible (see Fig.1 and 2). Furthermore, a special hybrid sigma coordinate will be developed for the ocean model with more realistic geography and topography.

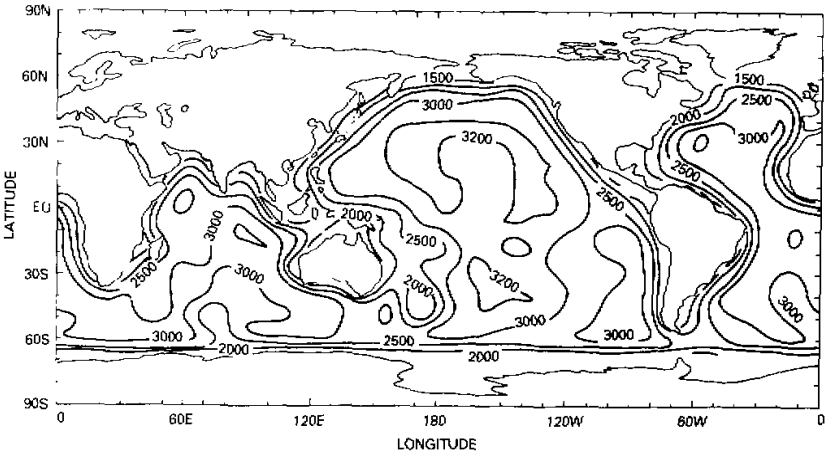

Fig.1. Model ocean depth.

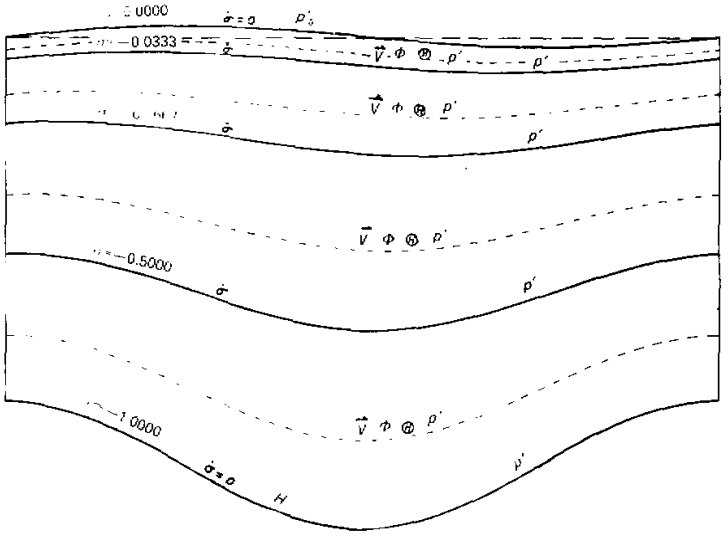

Fig.2. Vertical arrangement of variables in the sigma-coordinate system.

For the current version, the sigma vertical coordinate is defined as,

$$\sigma \equiv -\frac{z_0 - z}{z_0 + H} \qquad (z_0 \geqslant z \geqslant -H), \tag{16}$$

where $z_0 = z_0(\theta, \lambda, t)$ is the elevation of the sea surface, that is one of the prognostic variables of the model, and $H = H(\theta, \lambda)$ is the depth of the bottom.

Additionally, the method of variable substitution, preferable to design energy-conservation finite-difference schemes(Zeng and Zhang, 1982), is also used in the ocean model.

Let

$$\begin{cases} P \equiv \sqrt{\rho_0 g H}, \\ C_T = C_T(z) \equiv \sqrt{\dfrac{g\alpha_T}{\gamma_T}}, \\ C_S = C_S(z) \equiv \sqrt{\dfrac{g\alpha_S}{\gamma_S}}, \end{cases} \tag{17}$$

and

$$\begin{cases} \vec{V} \equiv P\vec{v}, \\ \Phi \equiv C_T P T', \\ \Theta \equiv C_S P S', \\ p'_0 \equiv \rho_0 g z_0, \\ P' \equiv \dfrac{\rho'}{\rho_0} P, \end{cases} \tag{18}$$

where $\gamma_T > 0$ and $\gamma_S > 0$ have been assumed. The equations of the model in coordinates $(\theta, \lambda, \sigma, t)$, with certain reasonable approximations, can be derived as,

$$\frac{\partial \vec{V}}{\partial t} = \alpha_1 \left[-L(\vec{V}) + A_M P \left(\Delta\vec{v} + \frac{1 - \mathrm{ctg}^2\theta}{a^2}\vec{v} + \frac{2\cos\theta}{a^2 \sin^2\theta}\vec{k} \times \frac{\partial \vec{v}}{\partial \lambda} \right) \right] + \beta \left[-f^* \vec{k} \times \vec{V} - \frac{1}{\rho_0}(P\Delta p' + 2\sigma P' P \nabla P) + \frac{\kappa}{H^2}\frac{\partial^2 \vec{V}}{\partial \sigma^2} \right], \tag{19}$$

$$\frac{\partial \Phi}{\partial t} = \alpha_2 \left[-L(\Phi) + \frac{\Phi}{C_T P^2}\frac{\partial C_T}{\partial \sigma}\left(P^2 \dot{\sigma} + (1+\sigma)\frac{\partial p'_0}{\partial t} + 2\sigma \vec{v} \cdot \nabla P \right) + A_H C_T P \Delta T' \right] + \beta \cdot \frac{\alpha_T}{C_T}\frac{P}{\rho_0}\left[P^2 \dot{\sigma} + (1+\sigma)\frac{\partial p'_0}{\partial t} + 2\sigma \vec{v} \cdot \nabla P \right] + \gamma_2 \frac{C_T P}{H^2}\frac{\partial}{\partial \sigma}\left(\frac{\kappa}{\delta}\frac{\partial (\tilde{T} + T')}{\partial \sigma} \right), \tag{20}$$

$$\frac{\partial \Theta}{\partial t} = \alpha_3 \left[-L(\Theta) + \frac{\Theta}{C_S P^2}\frac{\partial C_S}{\partial \sigma}\left(P^2 \dot{\sigma} + (1+\sigma)\frac{\partial p'_0}{\partial t} + 2\sigma \vec{v} \cdot \nabla P \right) + A_H C_S P \Delta S' \right] + \beta \cdot \frac{\alpha_S}{C_S}\frac{P}{\rho_0}\left[P^2 \dot{\sigma} + (1+\sigma)\frac{\partial p'_0}{\partial t} + 2\sigma \vec{v} \cdot \nabla P \right] + \gamma_3 \frac{C_S P}{H^2}\frac{\partial}{\partial \sigma}\left(\frac{\kappa}{\delta}\frac{\partial (\tilde{S} + S')}{\partial \sigma} \right), \tag{21}$$

$$\frac{\partial p'_0}{\partial t} = \delta_0 \cdot \left[-\frac{1}{a\sin\theta}\left(\frac{\partial PV\sin\theta}{\partial \theta} + \frac{\partial PU}{\partial \lambda} \right) - \frac{\partial P^2 \dot{\sigma}}{\partial \sigma} \right], \tag{22}$$

$$P' = -\frac{\alpha_T}{C_T}\Phi + \frac{\alpha_S}{C_S}\Theta, \tag{23}$$

$$\frac{\partial p'}{\partial \sigma} = -P'P. \tag{24}$$

where $L(F) \equiv \sum_{m=1}^{3} L_m(F)$ is the nonlinear operator, and α_1, α_2, α_3, β, γ_2, γ_3 and δ_0 are some flexible coefficients (Zeng and Zhang, 1987). In this paper, a certain kind of selections of the flexible coefficients will be used in developing speed–up algorithm for the ocean model.

III. BOUNDARY CONDITIONS AND ENERGY RELATIONS

1. *Boundary Conditions*

The boundary conditions fall naturally into two groups: (1) active or interactive boundary conditions at the sea surface, which is the interface between the ocean and the atmosphere and the continuity of pressure, stress, heat flux and salinity flux are required across this interface (Zeng, 1983); and (2) passive lateral and bottom boundary conditons, which determine the complex geometry boundary of the flows generated.

The sea surface is a free boundary, subject to the kinematic boundary condition given simply by

$$\dot{\sigma}\big|_{\sigma=0} = 0, \tag{25}$$

and the elevation of the surface, $z_0(\theta, \lambda, t)$, can be directly predicted by the model. Unlike most of the current OGCMs in the world, the surface gravity wave is not excluded from the model by the rigid–lid approximation (Bryan,1969). The restriction of the model's time step due to the presence of the high–speed waves, however, can still be relaxed by the technique of the flexible coefficients.

The pressure continuity condition at the surface may be given as,

$$p'\big|_{\sigma=0} = p'_s + p'_0, \tag{26}$$

where $p'_s \equiv p_s - \tilde{p_s}$ and p_s is the sea level air pressure.

At the surface, the main mechanisms driving the ocean are introduced in terms of fluxes of momentum, heat and salinity, hence the corresponding boundary conditions are as follows.

$$\frac{\kappa}{H}\frac{\partial \vec{v}}{\partial \sigma}\bigg|_{\sigma=0} = \frac{1}{\rho_0}\vec{\tau}, \tag{27}$$

$$\frac{\kappa}{H}\frac{\partial T}{\partial \sigma}\bigg|_{\sigma=0} = \frac{1}{\rho_0 c_p}F, \tag{28}$$

$$\frac{\kappa}{H}\frac{\partial S}{\partial \sigma}\bigg|_{\sigma=0} = \frac{S}{\rho_0}G, \tag{29}$$

where $\vec{\tau}$ is the surface wind stress, F the surface downward heat flux, and G the mass flux across the surface (in kg / m^{2}s) that will depend on the difference between the evaporation and precipitation rates(Crowley,1968). For fully coupled atmosphere–ocean models, $\vec{\tau}$, and G should be determined by both atmospheric and oceanic variables at the surface according to the bulk aerodynamic method(Zeng, 1983). In the simulations of the annual mean oceanic general circulation, which will be described in Section V, however, $\vec{\tau}$ will be given by using the observational annual mean wind stress (Han and Lee, 1981), and F will be taken as a simplified formula:

$$F = \rho_0 c_p \mu (T_a - T_s), \tag{30}$$

where T_a is the observational annual mean sea level air temperature, T_s the model's "sea surface temperature" and μ a relaxation factor with a scale of velocity (Bryan et al., 1979).

At the bottom, we have

$$\dot{\sigma}\big|_{\sigma=-1} = 0, \tag{31}$$

$$\frac{\partial \vec{v}}{\partial \sigma}\bigg|_{\sigma=-1} = 0, \tag{32}$$

$$\frac{\partial}{\partial \sigma}(T,\ S)\bigg|_{\sigma=-1} = 0. \tag{33}$$

At the side walls,

$$\vec{v}_n\big|_\Gamma = 0, \tag{34}$$

and

$$\frac{\partial}{\partial n}(T,\ S)\bigg|_\Gamma = 0, \tag{35}$$

where Γ is the lateral boundary and n represents the direction normal to Γ.

2. *Energy Relations and Available Energy Conservation*

So far, we have obtained a set of fundamental equations of the ocean model, which is very similar to that of IAP AGCM(Zeng et al, 1987). Therefore the integral properties, which should be maintained in approximate computations to avoid the false source or sink of mass and energy (Zeng and Zhang, 1987), can be derived immediately and the concept of the available energy can be introduced into the ocean model as well, which might be particularly useful because of the dramatic difference of the magnitude of order between kinematic energy and potential energy.

With the boundary conditions (25), (26) and (31)–(35), the equations of the model (19)–(24) possess following integral properties,

(1) *Total mass conservation*

$$\iint_S \frac{\partial p'_0}{\partial t}\, dS = 0, \tag{36}$$

where S represents the ocean area and $dS = a^2 \sin\theta d\theta d\lambda$;

(2) *Quadratic conservation of advective terms*

$$\int_{-1}^{0}\iint_{S} F \cdot L(F)dSd\sigma = 0, \tag{37}$$

where F may be U, V, Φ and Θ.

(3) *Relations of energy conversion*

$$\int_{-1}^{0}\iint_{S} \vec{V}\cdot\frac{P}{\rho_0}\nabla p'dSd\sigma = \int_{-1}^{0}\iint_{S}\left\{\frac{P}{\rho_0}\left(\frac{\alpha_I}{C_I}\Phi+\frac{\alpha_S}{C_S}\Theta\right)\left[P^2\dot{\sigma}+(1+\sigma)\frac{\partial p'_0}{\partial t}\right]\right\}dSd\sigma+\frac{\partial}{\partial t}\iint_{S}\frac{1}{2}(p'_0)^2dS, \tag{38}$$

where p'_s in (26) has been ignored.

Defining the available energy density as

$$e_a \equiv \frac{1}{2g}\left[|\vec{V}|^2+\Phi^2+\Theta^2+\frac{1}{\rho_0}(p'_0)^2\right], \tag{39}$$

we shall have the conservation of the gross available energy:

$$\frac{\partial}{\partial t}\int_{-1}^{0}\iint_{S} e_a dSd\sigma = 0. \tag{40}$$

if all the driving terms, dispersive terms and the terms related to vertical variation of stratifications are ignored in (20) and (21).

IV. NUMERICAL SCHEMES

1. *Arrangement of Variables*

In the vertical direction, $0 \geqslant \sigma \geqslant -1$, the model ocean is divided into four unevenly layers(see Fig.2) and prognostic variables, U, V, Φ, Θ, and the diagnostic variable p' are carried on the intermediate level of each layer, and the other two diagnostic variables, $\dot{\sigma}$ and p' on the layer interfaces (see Fig.2).

On every level, the scope of the world ocean is discreted by using the so-called C-grid system(Arakawa and Lamb, 1977) with the grid resolution of $\Delta\theta = 4^\circ$ and $\Delta\lambda = 5^\circ$. For the convenience to handle the rigid-wall boundary conditions, the variables are arranged in such a way that the $U(u)$ points are at the centers of the meridional faces of gridboxes and $V(v)$ points are at the centers of the latitudinal faces and all the other variables are carried on the centers of gridboxes.

2. *Spatial Finite-Difference Schemes*

All the finite-difference and average operators developed for IAP AGCM can be used in the present ocean model without any modification. For details, see Zeng and Zhang(1987).

3. *Time Integration Schemes*

The leap–frog method and Shuman's PGF average technique are used for all the processes in the model except for diffusive processes. To remove the time splitting that occurs slowly with the use of the leap–frog scheme a forward timestep is inserted at every model's month.

For the diffusive processes, the simple forward timestepping is employed.

V. ANNUAL MEAN SIMULATION

1. *Driving Fields, External Parameters and Initial Conditions*

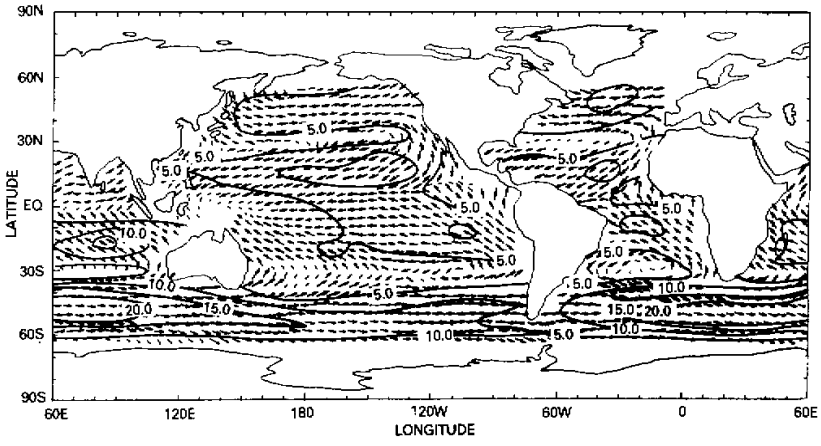

Fig.3. Observed annual mean sea level wind stress.

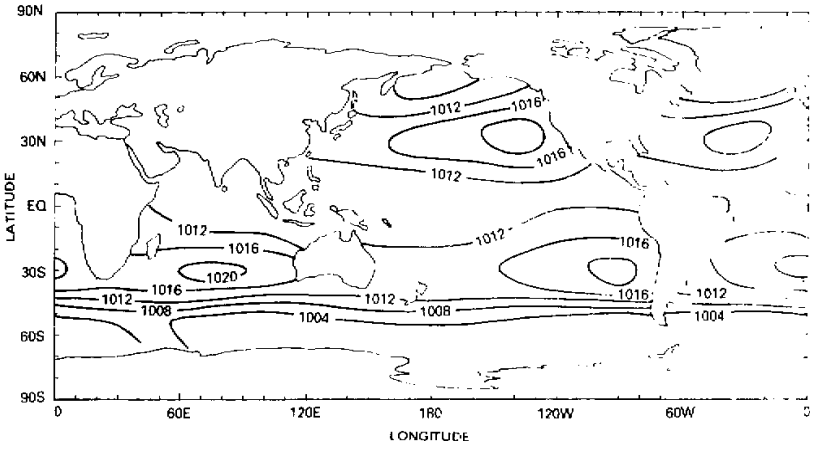

Fig.4. Observed annual mean sea level pressure (hPa).

Without taking into account of the variation of salinity temporarily, three external forcing fields, i.e., the wind stress $\vec{\tau}$, air pressure and temperature at the sea level are concerned in the present annual mean simulation(see Eqs. (27), (26) and (30)). Fig.3–5 show the annual mean distributions of these three atmospheric variables. There are two important external parameters in Eqs. (27), (28) and (30), i.e., the vertical eddy viscosity coefficient κ and the thermal relaxation factor μ, which determine the efficiency of the external forcings directly. In the present calculations, the values of κ and μ are set as, $\kappa = 1.0 \times 10^{-4}$ $m^2 s^{-1}$, and $\mu = 0.005 \sim 0.20$ m / day (see Table 2).

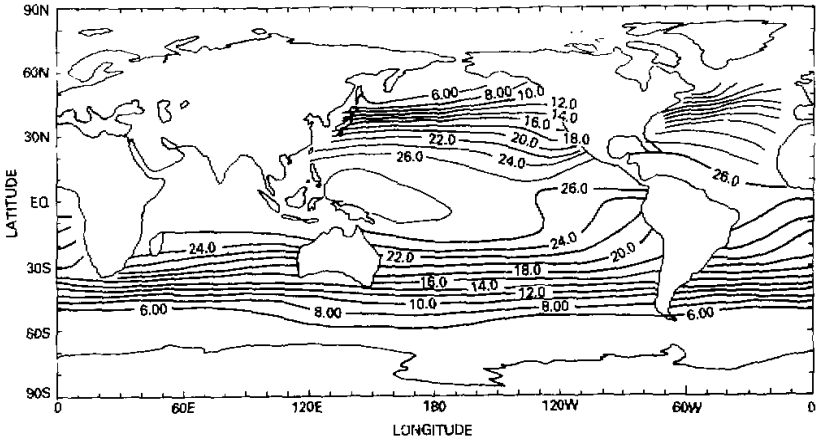

Fig.5. Observed annual mean sea level air temperature(deg. C).

Table 2. Values of Parameters in Time Period of Annual Mean Simulation

year	1–6	7–18	19–21	22	23
Δt^*	60	60	20	10	10
α_1	1	1	1	1	1
α_2	1	1	1	1	1
β	1 / 6	1 / 6	1 / 2	1	1
γ_3	3	3	1	1	1
δ_n	1 / 6	1 / 6	1 / 2	1	1
μ	0.05	0.05–0.20	0.20	0.20	0.05

* Δt is the time step (min.) of advective processes.

The annual mean simulation will start from a resting state with a flat sea surface and the standard vertical temperature profile. The corresponding initial condition may be written as.

$$\overline{V}^{(0)} = 0, \tag{41}$$

$$p'^{(0)}_{s} = 0, \tag{42}$$

and

$$\Phi^{(0)} = 0, \tag{43}$$

Eq. (43) implies that the standard temperature stratification has already been established at the beginning of integration, which would be more favourable to the downward heat transport than a uniform initial temperature distribution (e.g., see Bryan et al., 1979 and Han, 1984).

2. *Accelerating Convergence Algorithm*

The ocean, as pointed out by Bryan(1984), represents a broad-banded system with a frequency-range order of magnitude greater than the atmosphere. The time required for the ocean to adjust to external boundary conditions is of the order of 1000 years. On the other hand, many of the high frequency processes (e.g., the surface gravity wave and internal gravity waves) are contained in the ocean. It is obviously impractical to force ocean models to equilibrium by normal time integration methods. As a matter of fact, an artificial device based on the so-called "distorted physics" (Bryan, 1984) has been being used for speeding up the convergence of the solution to equilibrium in a steadily forced and frictionally controlled ocean (Semtner, 1973, Bryn et al., 1979 and Han, 1984). One of the explanations for such a device is that the frequency bandwidth of the ocean system is reduced towards the end of lower frequencies, which are dominant in the band, for certain cases such as steadily forcing processes.

Stimulated by the technique mentioned above, a slightly different accelerating convergence algorithm, based on the flexible coefficients, is used in the present calculation. The coefficients, α, β, γ, δ, in Eqs. (19)-(22), which should be 1.0 in a normal case, are set as different values in the first eighteen years of the integration (see Table 2). In doing so, different timesteps are given to different physical processes: the time steps are one hour for advective processes, one sixth hour for the processes of energy conversion, and three hours for the vertical heat transport process respectively. The basic idea of such an unsychronous time integration technique is the same as mentioned above. However, the main features of the present algorithm exist in the following two aspects:

(1) the unsynchronous treatment is used for not only the different equations of the model, but also the different terms of each equations, which characterize different physical processes;

(2) the use of the flexible coefficients makes the present algorithm free of false computational source and sink of energy and mass(for details see Zeng et al., 1982).

By using the accelerating algorithm, a twenty-three year's simulation with annual mean forcing conditions has been performed. Fig. 6 shows the temporal variations of the temperatures averaged over the sea area for all the model's levels. It can be seen that the variations are approaching to steady states, especially at the depth of 50m and 300m. By the twenty-second year, the increase of the temperature are 3.7 ° C, 5.0 ° C, 1.8 ° C and 0.5 ° C for 50m, 300m, 1000m and 2000m depths respectively, that implies the downward heat transport in the model is significant during that time period.

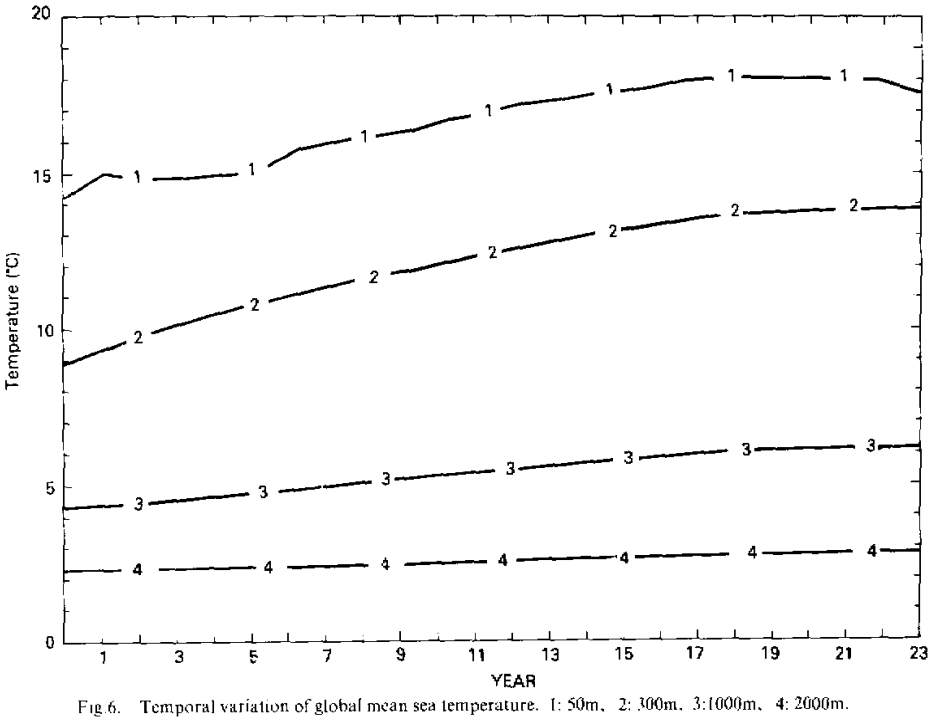

Fig.6. Temporal variation of global mean sea temperature. 1: 50m, 2: 300m, 3:1000m, 4: 2000m.

3. *Simulated Annual Mean Fields*

(1) *Currents*

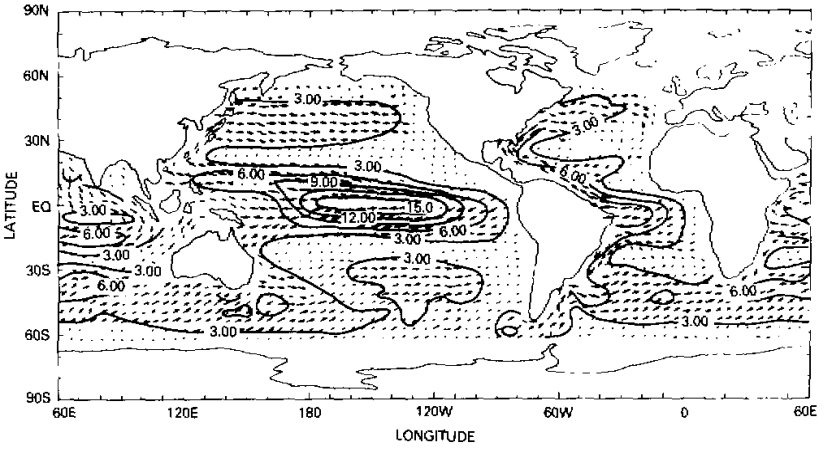

Fig.7. Ocean current (cm / s). Depth 50m Year=23.

Fig.7 shows the simulated surface currents at the depth of 50m. In contrast to the wind stress field, it is very clear that the Ekman transport exerts a dominant effect on the large-scale surface current pattern. The major western boundary intensification phenomena can be seen in the model's simulation although their speeds are much weaker than the observed ones. The failure of the model in the simulation of some observed narrow currents such as the equatorial countercurrents might be related to the coarse resolution of the present model.

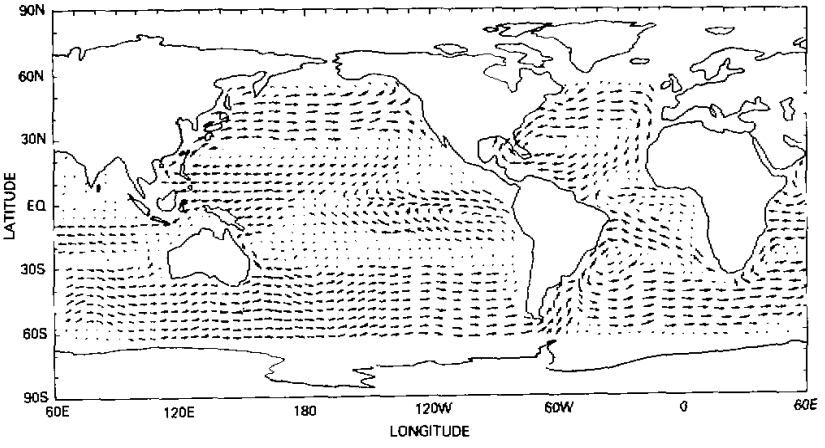

Fig.8. Ocean current (cm / s). Depth 300m Year-23.

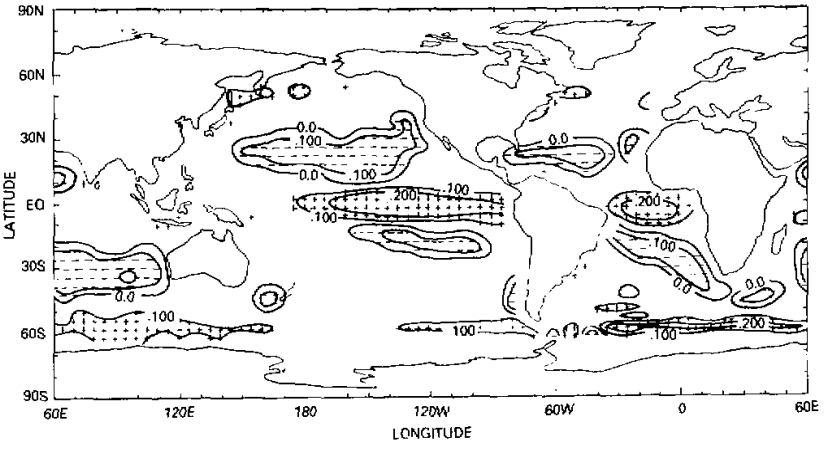

Fig.9. Vertical velocity. Depth 100m Year-8.

The subsurface currents simulated at level 2 (300m depth) are shown in Fig.8. Interesting equatorial features in the central and eastern Pacific and Atlantic Oceans are the eastward-flowing equatorial undercurrents and the associated equatoriward convergence.

The vertical velocities computed at the bottom of the surface layer are shown in Fig. 9. The strong upwilling in a narrow band along the equator and the downwelling immediately to the north and south concur with the patterns of convergence and divergence at the subsurface layer and the surface layer.

The simulated current at level 4 (2000m) are displayed in Fig.10, in which one of interesting features is the western boundary countercurrents with respect to the surface boundary current.

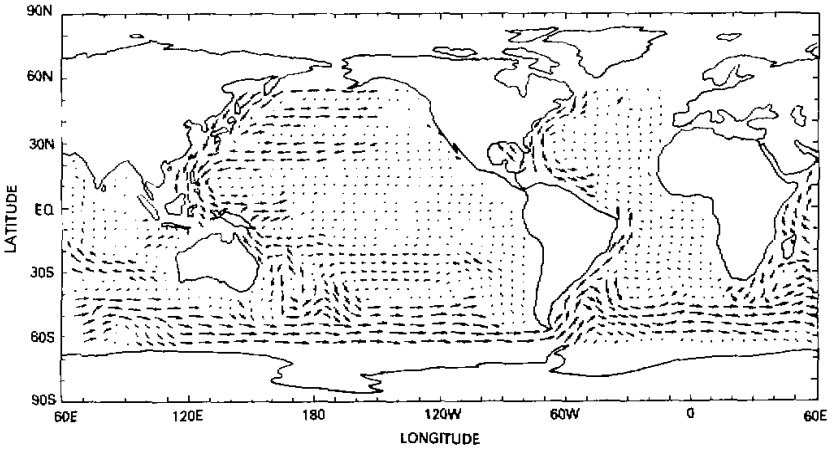

Fig.10. Ocean current (cm / s). Depth 2000m Year-23.

(2) *Temperature*

Fig. 11 shows the simulated surface layer temperature in the twenty-second year. It is clear that the formation of the sea surface temperature is mainly concerned to the process of the linear response of the sea temperature to the sea level atmospheric temperature (see Fig.5). The small-scale noise appearing in the northern and southern boundary regions(see Fig. 11) might be due to the lack of suitable filtering device in the present model.

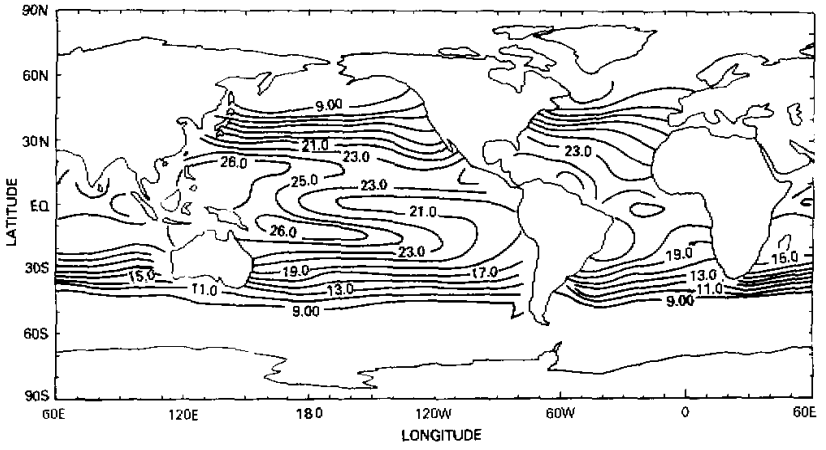

Fig.11. Sea temperature. Depth 50m Year=22 deg.C.

(3) *Surface elevation*

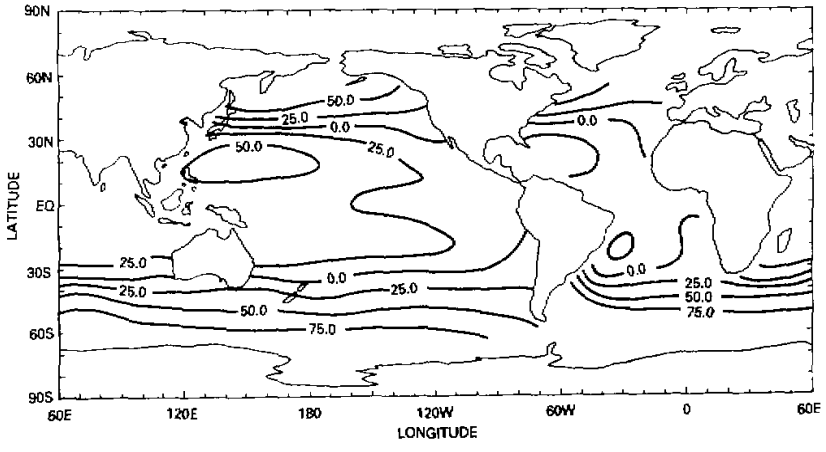

Fig.12. Sea surface elevation in cm. Year=22.

The simulated sea surface elevation is shown in Fig.12. The highest region of the elevation is in the west Pacific Ocean and the lowest region is around the Antarctica. It is notable that the order of magnitude of the available surface potential energy determined by the surface elevation is the same as that of the kinematic energy. We speculate, therefore, that the effect of the pressure gradient caused by the fluctuation of the sea surface on the surface layer currents is not ignorable.

The present research work was performed during the authors' visit in the Laboratory for Planetary Atmospheres

Research at SUNY at Stony Brook in the United States. We are in debt to Dr. Robert D. Cess and Dr. Sultan Hameed for their considerable help and benificial discussions. We thank Sanjay Kapur, Kenneth Sperber, Bill Persons, Leonard Boyle, Dr. David Zhou, Dr. Louis Vaz and Dr. John Milazzo for their help in using the computers. We also thank Chen Shengfang for typing the manuscript.

This work was supported by the CO_2 Research Division, Office of Basic Energy Sciences, United States Department of Energy, under Grant DEFG0285ER60314 to SUNY at Stony Brook.

REFERENCES

Arakawa, A. (1966). Computational design for long-term numerical integration of the equations of fluid motion: Two dimensional incompressible flow, Part I, *J. Comp. Phys.*, **1**: 119-143.

Arakawa, A., and V.R. Lamb (1977). Computational design of the basic dynamical processes of the UCLA general circulation model. In *Methods in Computational Physics*, Vol. 17, General Circulation of the Atmosphere, J. Chang(Ed.), Academic Press, New York, 173-265.

Bryan,K. (1969). A numerical method for the study of the circulation of the world ocean, *J. Comp. Phys.*, **3**: 347-376.

Bryan, K., and M. Cox (1972). An approximate equation of state for numerical models of ocean circulation, *J. Phys. Oceanogr.*, **2**: 510-514.

Bryan, K., S. Manabe and R.C. Pacanowski (1975). A global ocean-atmosphere climate model, Part II. The oceanic circulation, *J. Phys. Oceanogr.*, **5**: 30-46.

Bryan, K., and L.J. Lewis (1979). A water mass model of the world ocean, *J. Geophs. Res.*, **84**: 2503-2517.

Bryan, K. (1984). Accelerating the convergence to equilibrium of ocean-climate models, *J. Phys. Oceanogr.*, **14**: 666-673.

Charney, J.G., and G.R. Flierl (1981). Oceanic analogues of large-scale atmospheric motions. In *Evolution of Physical Oceanography*, Warren, B.A. and Wunsch, C.(Ed.), The MIT Press, Cambridge, Massachusetts and London, England, 504-548.

Crowley,W.P. (1969). A global numerical ocean model, Part I, *J. Comp. Phys.*, **3**: 111-147.

Eckart, C. (1958). Properties of water, Part II. *Am. J. Sci.*, **256**: 225-240.

Gates, W.L., and A.B. Nelson (1975). A new (revised) tabulation of the scripps topography on a 1° global grid, Part II, Ocean depths. R-1277-1-ARPA, The Rand Corporation, Santa Monica, CA, 132pp.

Han, Y.-J., and Lee, S.-W. (1981). A new analysis of monthly mean wind stress over the global ocean, Report No. 26, Climatic Research Institute, Oregon State University, Coroallis, 148pp.

Han, Y.-J. (1984). A numerical world ocean general circulation model, Part II, A baroclinic experiment, *Dyn. Atmos. Oceans*, **8**: 141-172.

Phillips, N. (1956). The general circulation of the atmosphere: A numerical experiment. *Quart. J. Meteorol. Soc.*, **82**: 123-164.

Smagorinsky, J. (1963). General circulation experiments with the primitive equations, I. The basic experiment. *Mon. Wea. Rev.*, **93**: 99-164.

Semtner, A.J. (1986). History and methodology of modelling the circulation of the world ocean, In *Proceedings of the NATO Advanced Study Institute on Advanced Physical Oceanographic Numerical Modelling*, D. Riedel Publishing Co., Dordrecht, 23-32.

Zeng, Q. C., Z. Z. Ji and C. G. Yuan (1982). Design of difference schemes for the primitive equations, *Scientia Sinica*, Series B, Vol. XXV, No.2, 183-199.

Zeng, Q. C. (1983). Some numerical ocean-atmosphere coupling models, *Proceedings of the First International*

Symposium on Integrated Global Ocean Modelling. Tullin. SSSR.

Zeng, Q. C., and X. H. Zhang (1982), Perfectly energy-conservative time-space finite-difference schemes and the consistent split method to solve the dynamical equations of compressible fluid. *Scientia Sinica*, Series B. Vol. XXV, No.8, 866-880.

Zeng, Q. C., C. G. Yuan, X. H. Zhang, X. Z. Liang and N. Bao (1987), A global gridpoint general circulation model. In *Collection of Papers Presented at the WMO / IUGG NWP Symposium*, Tokyo, 4-8 August 1986, 421-430.

Zeng, Q. C., and X. H. Zhang (1987), Available energy conservative finite- difference schemes for baroclinic primitive equations on spere, *Chinese Journal of Atmospheric Sciences*. Vol. 11, No. 2, 121-142.